J. Phycol. **41,** 126–139 (2005)

DOI: 10.1111/j.1529-8817.2005.04080.x

MORPHOMETRIC TAXONOMY OF SIPHONOUS GREEN ALGAE: A METHODOLOGICAL STUDY WITHIN THE GENUS *HALIMEDA* (BRYOPSIDALES)[1]

Heroen Verbruggen,[2] *Olivier De Clerck, Ellen Cocquyt*

Phycology Research Group and Center for Molecular Phylogenetics and Evolution, Ghent University, Krijgslaan 281 (S8), B-9000 Gent, Belgium

Wiebe H. C. F. Kooistra

Stazione Zoologica "Anton Dohrn," Villa Comunale, 80121 Naples, Italy

and

Eric Coppejans

Phycology Research Group, Ghent University, Krijgslaan 281 (S8), B-9000 Gent, Belgium

Species-level taxonomy of Bryopsidalean genera is often based on quantifiable morphological characters. Yet there are relatively few examples of statistically founded morphometric studies within this group of siphonous algae and macroalgae in general. Molecular phylogenetic studies have revealed cases of cryptic diversity in several Bryopsidalean genera and call for new approaches toward taxonomy. We present a combined molecular and morphometric approach toward *Halimeda* taxonomy using a selection of specimens representing the five natural lineages within the genus. A phylogeny was inferred from partial nuclear rDNA sequences (3′ end of small subunit, internal transcribed spacer region 1, 5.8S, internal transcribed spacer region 2, and 5′ end of large subunit) from our and previously studied specimens. Segment size and shape descriptors were acquired using different techniques, including landmark analysis and elliptic Fourier analysis. A broad range of anatomical structures was measured. Taxonomic utility of the different methods and characters was assessed using predictive discriminant analysis. Molecular data were used to delimit species groups. Segment morphological characters proved fairly good predictors for species membership, but anatomical variables yielded the best results. The good performance of morphometric taxon predictors offers perspectives, not only for future taxonomic case studies within problematic species complexes, but also for thorough examinations of the rich fossil record of *Halimeda*. Statistically founded morphometric studies can probably help elucidate taxonomic issues within other Bryopsidalean genera as well.

Key index words: **anatomy; Bryopsidales; *Halimeda*; morphology; morphometrics; phylogeny; siphonous algae; taxonomy**

Abbreviations: **DA, discriminant analysis; EFA, elliptic Fourier analysis; ITS, internal transcribed spacer; TBR, tree bisection-reconnection**

Morphometric analysis, the mathematical investigation of shape, allows objective and statistically sound evaluation of morphological variation to answer a broad spectrum of biological questions. Macroalgae are at first sight less suited for morphometric investigation because their structures and branching patterns are marked by considerable stochastic variation and plasticity. Contrary to botanists and zoologists, phycologists do not have the habit of embracing morphometrics to answer their taxonomic and ecological questions. Nonetheless, during the last 5 years, a raise in interest for morphometrics could be observed (Sherwood and Sheath 1999, Kraan et al. 2001, Krellwitz et al. 2001, Collado-Vides 2002, Hubbard and Garbary 2002, Vieira and Necchi 2002, de Senerpont Domis et al. 2003, Kamiya et al. 2003, Vroom and Smith 2003, Vroom et al. 2003, Haywood et al. 2004, Murray et al. 2004). Achievements of these studies include reports of morphological differences between taxa and the description of taxon boundaries.

In the present study, we explore the taxonomic utility of morphometric methods in the genus *Halimeda*. This genus belongs to the Bryopsidales, a group of algae characterized by siphonous thalli, each specimen essentially comprising a single giant multinucleate cell. The siphons branch, anastomose, and adhere to form very simple (e.g. *Derbesia*, *Bryopsis*) to highly complex (e.g. *Avrainvillea*, *Halimeda*) thalli. Within genera, direct observations of thallus shape and a limited number of anatomical characters and measurements are

[1]Received 26 May 2004. Accepted 8 October 2004.
[2]Author for correspondence: e-mail heroen.verbruggen@ugent.be.

supposed to lead to accurate taxonomic assignment. However, recent molecular studies showed morphological convergence and cryptic diversity (Kooistra 2002, Kooistra et al. 2002); that is, genetically distinct species cannot be keyed out with current procedures and insights in morphology. Yet these classical approaches may not use the anatomical and morphological information to the fullest.

The genus *Halimeda* is a particularly interesting target for morphometric studies because its thalli are composed of calcified segments with a particular shape (Fig. 1, a and b), and many anatomical structures can be quantified. Within segments, an inner medulla and an outer cortex can be discerned (Fig. 1, e–h). Medullar siphons are oriented along the thallus axis and string the segments together. These siphons branch laxly, with the main branch continuing toward the thallus apex and side branches giving rise to the cortex (Fig. 1, g and h). In the cortex, siphon branching is denser. This results in several layers of short, often in-

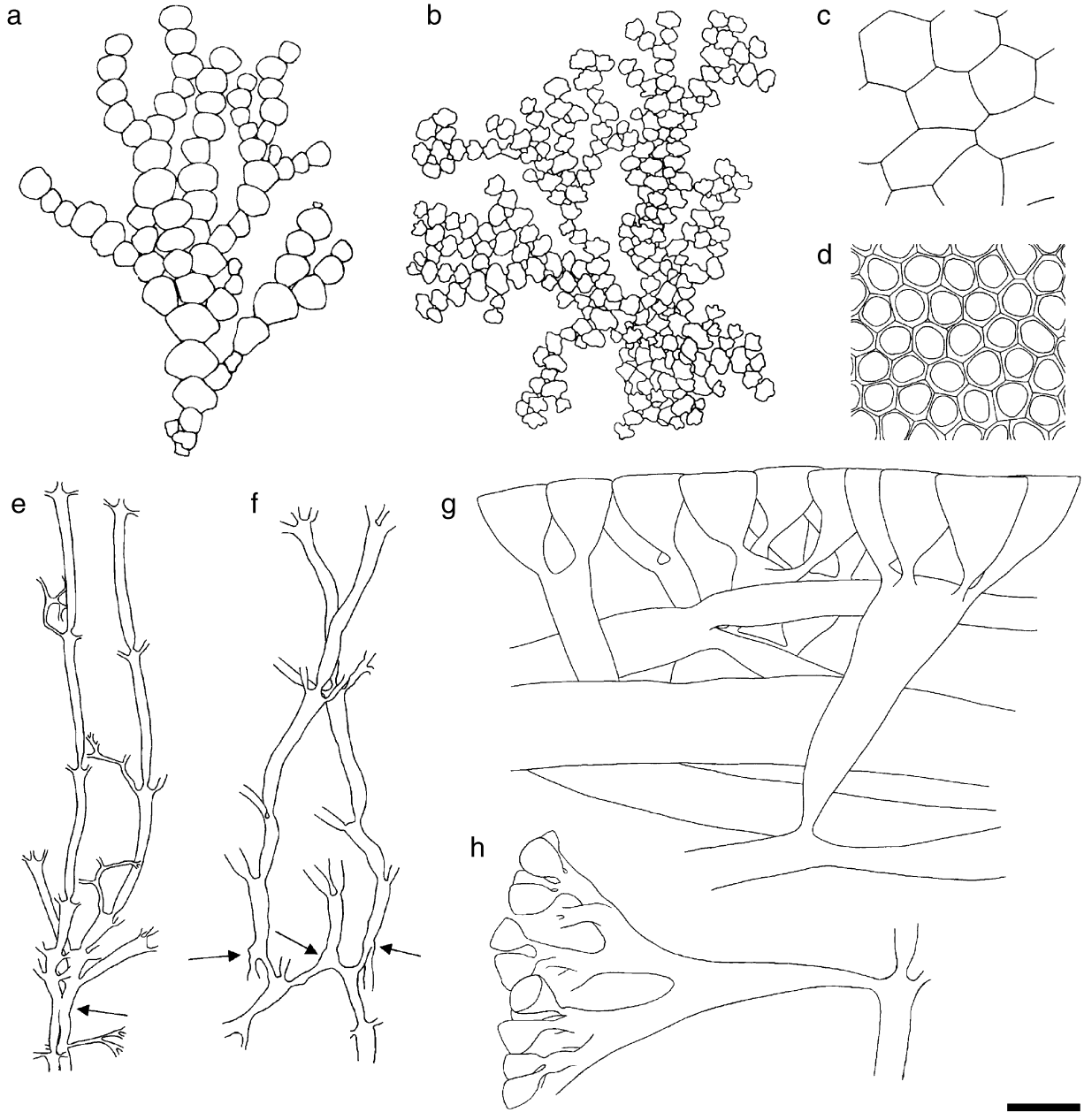

FIG. 1. Thallus morphology and anatomical details of a few *Halimeda* species used in this study. (a–b) Thallus morphology. (a) *H. lacunalis*, HV306-1. (b) *H. gracilis*, C&PvR13865B. (c–d) Surface view. (c) *H. tuna*, HV54. (d) *H. gracilis*, HV317. (e–f) Medulla and nodal region. (e) *H. opuntia*, HV19. (f) *H. tuna*, HV54. (g–h) Cortical region in cross-section. (g) *H. tuna*, HV54. (h) *H. micronesica*, WLS184-02. Arrows indicate the location of the node. Scale bars: 25 mm for thalli, 400 μm for medulla, 60 μm for cortical structures and surface views. All species deposited in GENT. (Adapted from Verbruggen and Kooistra 2004.)

flated siphons called utricles. Peripheral utricles adhere (Fig. 1, c, d, g, and h) and enclose an intersiphonal space where aragonite precipitation occurs (Borowitzka and Larkum 1977).

Classical morphotaxonomy discerned 35 species in five sections (Dong and Tseng 1980, Hillis-Colinvaux 1980, Ballantine 1982, Noble 1986, Kraft 2000). Although sections were defined on the basis of patterns of siphon fusion at nodes between segments, species recognition within sections was primarily based on segment shape and cortical patterns. This taxonomy has been questioned by molecular phylogenetic studies based on partial rDNA sequence analysis. The evolutionary partitioning of the genus proved different from Hillis-Colinvaux' (1980) sectional subdivision (Verbruggen and Kooistra 2004), and several nonmonophyletic species and cases of cryptic diversity within species were revealed (Kooistra et al. 2002).

The phylogenetic insights resulted in a revision of the sectional subdivision, which is now in accordance with major evolutionary directions within the genus. Each of the new sections can easily be recognized by unique combinations of synapo- and symplesiomorphies (Kooistra et al. 2002, Verbruggen and Kooistra 2004). Within lineages, some species can be easily recognized, whereas other species lump into morphocomplexes with or without internal molecular phylogenetic structure. In addition to the previously mentioned cases of nonmonophyly and hidden diversity, additional taxonomic problems occur (Noble 1987, Dargent 1997). Specimens are often difficult to identify with existing identification keys and taxonomic descriptions. This is probably due to a combination of three factors. First, traditional qualitative characters generally are not diagnostic for closely related species. Second, intraspecific morphological plasticity appears to be underestimated. Finally, there seems to exist a historical bias of taxonomy toward Caribbean species, with Indo-Pacific representatives fitted in without full consideration of morphological variation. A new approach toward the taxonomy of the genus is sorely needed.

Here we explored the utility of a combined molecular and morphometric approach toward species separation in *Halimeda*, using a limited number of specimens representing the five natural lineages within the genus. We aimed 1) to estimate the feasibility of morphometric taxonomy within the genus, 2) to gain insight in the taxonomic utility of different morphometric methods and characters at different taxonomic levels, 3) to narrow the range of techniques and measurements for future case studies within morphological species complexes, and 4) to discuss the potential of morphometric taxonomy in Bryopsidalean algae.

The first two issues were tackled by comparing the adequacy of clade membership prediction by a series of morphometrics (quantitative morphological characters) taken from segments and anatomical structures. Molecular information was used as an objective allocator of specimens to species-level groups; in other words, the species groups used were delimited on the basis of objective sequence data. Segment size and shape were digitized using landmark methods (Rohlf and Marcus 1993) and outline analysis (elliptic Fourier analysis [EFA]; Kuhl and Giardina 1982). The third question was raised when dissecting segments and measuring their anatomical structures proved to be extremely time consuming. To approach this issue, the behavior of central and deviance measures of anatomical variables were examined in the light of specimen and segment sampling approaches. In a parallel study (Verbruggen et al. 2005), we reported on the exploratory statistics and so-called deviant segments and their influence on group membership prediction.

MATERIALS AND METHODS

Species sampling. Nine species were sampled covering the phylogenetic spectrum of the genus. From each of the large sections (*Rhipsalis*, *Halimeda*, and *Opuntia*), two or three species were chosen; from smaller sections (*Micronesicae* and *Pseudo-opuntia*), a single species was selected. Morphological species identifications were based on Hillis-Colinvaux (1980). For each species, two or three specimens were examined (Table 1). All specimens are deposited in the Ghent University Herbarium, Belgium (GENT).

Sequence analysis. DNA was extracted and amplified as described in Kooistra (2002). Sequences of the nuclear rDNA region were obtained (3′ end of 18S, internal transcribed spacer [ITS] region 1, 5.8S, ITS2, and 5′ end of 28S) following procedures in Kooistra (2002). Of specimens HV46b and H.0257, only partial sequences could be obtained. For HV46b it concerns ITS1, 5.8S, ITS2, and the 5′ end of 28S; for H.0257 it concerns the 3′ end of 5.8S, ITS2, and the 5′ end of 28S. For specimen HV45, we were unable to obtain a sequence. Forward and reverse sequences were merged using Autoassembler, version 1.4.0 (Applied Biosystems Foster City, CA, USA). Obtained sequences were added to the alignment of Kooistra (Kooistra et al. 2002, Verbruggen and Kooistra 2004) and were aligned manually in BioEdit, version 5.0.9 (Hall 1999). Unweighted maximum parsimony trees were inferred from the obtained alignment of specimens in Tables 1 and 2 using PAUP*, version 4.0.b10 (Swofford 2001) using the TBR branch-swapping algorithm. Gaps were treated as missing data, and starting trees were obtained via stepwise addition. Sequences of *Udotea flabellum* (Ellis and Solander) Howe and *Penicillus capitatus* Lamarck were used as outgroup (Kooistra et al. 2002, Verbruggen and Kooistra 2004). Bootstrap support (100 replicates) was obtained under the same criteria as the heuristic maximum parsimony analysis.

Morphometrics. Segment sampling: For morphometric examination of small specimens (less than about 100 segments) all segments were investigated. Of larger thalli, between 48 and 89 segments were sampled in series spanning the entire thallus length. For sprawling species (*H. gracilis* and *H. opuntia*), the basal reference segment was arbitrarily chosen.

Thallus structure: The position of segments within the thallus was determined as the distance of the segment to the basal segment (number of intermediate nodes). Segments were classified into three groups according to their location along the thallus axis: the lowermost 25% (thal_prt = 1), the central 50% (thal_prt = 2), and the uppermost 25% (thal_prt = 3). The binary variable apical was set to 1 for apical segments or 0 for nonapical segments. Noted was also whether segments were calcified or not. The local branching pattern was characterized by counting the number of sister segments and the number of daughter segments.

TABLE 1. Specimens in the morphometric study.

Section	Species	GENT	Geographic origin	Ocean	GenBank
Rhipsalis	*H. borneensis*	HV18-1	Zanzibar Island (Tanzania)	Western Indian	AY786512
		HV183b	Tahiti, French Polynesia	Central Pacific	AY786513
	H. macroloba	HV38	Zanzibar Island (Tanzania)	Western Indian	AY786514
		HV45	Mnazi Bay, Tanzania	Western Indian	—
		HV206	Tahiti, French Polynesia	Central Pacific	AY786515
Micronesicae	*H. micronesica*	H.0014-1	Great Barrier Reef, Australia	Western Pacific	AY786516
		WLS184-02	Wallis Island (France)	Central Pacific	AY786517
		WLS420-02	Wallis Island (France)	Central Pacific	AY786518
Halimeda	*H. lacunalis*	HV306-1	Rangiroa, French Polynesia	Central Pacific	AY786519
		HV308-1	Rangiroa, French Polynesia	Central Pacific	AY786520
	H. taenicola	HV285-1	Rangiroa, French Polynesia	Central Pacific	AY786521
		HV285-2	Rangiroa, French Polynesia	Central Pacific	AY786522
		HV306-3	Rangiroa, French Polynesia	Central Pacific	AY786523
	H. tuna	H.0113-1	Naples, Italy	Mediterranean Sea	AF407248
		HV319	Rosas, Spain	Mediterranean Sea	AY786524
Pseudo-Opuntia	*H. gracilis*	HV312-1	Rangiroa, French Polynesia	Central Pacific	AY786525
		HV317-1	Rangiroa, French Polynesia	Central Pacific	AY786526
Opuntia	*H. goreauii*	H.0257	Bocas del Toro, Panama	Caribbean Sea	AY786527
		H.0258-1	Galeta, Panama	Caribbean Sea	AF525610
	H. opuntia	HV46b	Mnazi Bay, Tanzania	Western Indian	AY786528
		HV61	Moorea, French Polynesia	Central Pacific	AY649380

Given are their accession number in the GENT herbarium, geographic origin, and GenBank accession number of their nuclear rDNA sequences.

Segment morphology: Segment form was digitized from calibrated digital pictures of various thallus parts. After being numbered, individual segments were aligned horizontally with their base pointing downward (Fig. 2, a and b).

Categorical shape variables: From the segment pictures, a first set of six variables (Table 3: s7–s12) corresponding to characters traditionally used in taxonomic treatises of *Halimeda*, was gathered for specimens HV18-1, HV206, WLS184-02, HV285-1, HV319, HV312-1, H.0257, and HV46b.

Conventional measurements: Five landmarks were digitized using tpsDIG (version 1.31, Rohlf 2001a). Two landmarks were placed on the right and left sides of the segment's attachment zone (Fig. 2a); three more were placed at the left, top, and right extremities of the segment.

The following conventional size variables (segment length and width, the height where the width is maximal, and width of the attachment zone, variables s13–s17) were calculated from the landmark coordinate files using the following equations (visualized in Fig. 2b).

$$\text{length} = y4 - \frac{y1 + y2}{2}$$

$$\text{width} = x5 - x3$$

$$\text{homw} = \frac{y3 + y5}{2} - \frac{y1 + y2}{2}$$

$$\text{attach} = \sqrt{(y1 - y2)^2 + (x1 - x2)^2}$$

Segment thickness was measured using calipers. The five conventional variables presented a lognormal distribution and were transformed using the neperian logarithm (ln) for all analyses that required it.

Ratio shape variables: Using untransformed size variables, five ratios expected to provide useful segment shape information were calculated: segment length over segment width, width of attachment zone over segment width, height of maximal segment width over segment length, segment thickness over segment length, and segment thickness over width of attachment zone (Table 3, s18–s22).

Landmark analysis: We carried out a geometric landmark analysis (Bookstein 1989, 1991, Rohlf and Marcus 1993) on the group of landmarks described above. This type of analysis extracts the variation in geometric configuration of a set of landmarks that are superimposed on each of the specimens and codes this variation in a series of continuous variables (partial warps). The whole analysis up until the extraction of partial warp scores was performed with tpsRELW (version 1.31, Rohlf 2001b). Landmark configurations were aligned using the general orthogonal least-squares method (Rohlf and Slice 1990). The configuration of averaged landmarks was chosen to be the point of tangency between Kendall's shape space and tangent space (Rohlf et al. 1996). The relation between Procrustes distances and the linear distances in tangent space was evaluated for linearity using tpsSMALL (version 1.19, Rohlf 1998). Partial warp scores were computed with alpha set to zero so as not to weigh the principal warps (Rohlf 1993). Uniform shape changes (s23 and s24) were computed following Bookstein (1996). Nonuniform, localizable shape changes are coded in variables s25–s28.

Elliptic Fourier analysis: In EFA (Kuhl and Giardina 1982), shape characteristics of the outline of the studied object are translated into mathematical variables. The resulting number of variables is proportional to the desired degree of precision between the original outline and the closed contour captured in the variables. Segment outlines were traced manually from the aligned segment images. The outlines were then rotated 90 degrees clockwise to facilitate their digitization using the center of the attachment zone as a fixed starting point (tpsDIG version 1.31, Rohlf 2001a). All points along the segment outlines were saved. Visual inspection of the degree to which outlines reconstructed from Fourier coefficients corresponded to the original outlines (EFAWin, Isaev 1995), suggested that 10 harmonics captured the major shape properties of the segments. Coefficients for 10 harmonics were extracted with Morpheus et al. (Slice 2000). The Morpheus et al. software was set to remove size differences. Rotational correction was omitted because the visual alignment already present in the outline pictures was more pleasing. The program was set to use the first coordinate couple as

TABLE 2. List of previously published sequences used in our phylogeny.

Species	GENT	Geographic location	Ocean	GenBank
H. borneensis	HEC12603b	Zanzibar, Tanzania	Western Indian	AF525559
H. borneensis	H.0267	New Caledonia	Western Pacific	AF525550
H. melanesica	no voucher	Taka Garlarang, Indonesia	Western Pacific	AF407237
H. incrassata IP	PH197	Cebu, Philippines	Western Pacific	AF407241
H. incrassata IP	H.0045	Rangiroa, French Polynesia	Central Pacific	AF525573
H. macroloba	H.0157	Pangasinan, Philippines	Western Pacific	AF525560
H. macroloba	H.0038	Tahiti, French Polynesia	Central Pacific	AF525563
H. cylindracea	SOC364	Socotra, Yemen	Western Indian	AF525546
H. cylindracea	H.0018	Great Barrier Reef, Australia	Western Pacific	AF525548
H. simulans	H.0367	Panama	Caribbean Sea	AF407235
H. incrassata CAR	H.0181	Florida, USA	Caribbean Sea	AF525537
H. incrassata CAR	H.0179	Bahamas	Caribbean Sea	AF407233
H. monile	H.0228	Yucatan, Mexico	Caribbean Sea	AF407234
H. cryptica	H.0237	Discovery Bay, Jamaica	Caribbean Sea	AF407244
H. micronesica	no voucher	Great Barrier Reef, Australia	Western Pacific	AF407243
H. fragilis	H.0125	Bile Bay, Guam	Western Pacific	AF407245
H. hummii	H.0253	San Blas, Panama	Caribbean Sea	AF525581
H. discoidea ATL	H.0207	Gran Canaria, Canary Islands	Eastern Altantic	AF407249
H. tuna MED	H.0113	Naples, Italy	Mediterranean Sea	AF407250
H. tuna ATL	H.0231	Puerto Morelos, Mexico	Caribbean Sea	AF407248
H. lacunalis	H.0121	Agat Bay, Guam	Western Pacific	AF525579
H. magnidisca	SOC252	Socotra, Yemen	Western Indian	AF525595
H. magnidisca	SOC348	Socotra, Yemen	Western Indian	AF525596
H. discoidea IP	SOC299	Socotra, Yemen	Western Indian	AF407254
H. discoidea IP	H.0041	Moorea, French Polynesia	Central Pacific	AF525604
H. taenicola	H.0037	Tahiti, French Polynesia	Central Pacific	AF407255
H. cuneata	no voucher	W Australia	Eastern Indian	AF525606
H. macrophysa	H.0271	New Caledonia	Western Pacific	AF525590
H. gigas	H.0122	Cocos Island, Guam	Western Pacific	AF407252
H. gracilis IP	HEC11839	Beruwala, Sri Lanka	Central Indian	AF407257
H. lacrimosa	H.0308	Bahamas	Caribbean Sea	AF407258
H. gracilis CAR	H.0405	Isla Grande, Panama	Caribbean Sea	AF525609
H. minima	SOC384	Socotra, Yemen	Western Indian	AF407263
H. minima	PH526	Mindanao, Philippines	Western Pacific	AF525618
H. minima	H.0382	Apra Harbor, Guam	Western Pacific	AF407265
H. renschii	C&PvR13855B	Madang, Papua New Guinea	Western Pacific	AF407262
H. opuntia	H.0262	Tamandare, Brazil	Western Atlantic	AF525639
H. opuntia	HEC12584	Zanzibar, Tanzania	Western Indian	AF525629
H. distorta	no voucher	Cebu, Philippines	Western Pacific	AF525652
H. distorta	H.0280	New Caledonia	Western Pacific	AF525641
H. hederacea IP	H.0475	Great Barrier Reef, Australia	Western Pacific	AF407269
Penicillus capitatus	H.0349	San Blas, Panama	Caribbean Sea	AF407271
Udotea flabellum	H.0415	Portobelo, Panama	Caribbean Sea	AF407270

For specimens housed in the Ghent University herbarium, their accession number in this herbarium is given. For the biphyletic species (see Kooistra et al. 2002), the geographic origin is indicated after the species epitaph: CAR, Caribbean; ATL, Atlantic; IP, Indo-Pacific; MED, Mediterranean.

a fixed starting point. All 40 variables resulting from the analysis (four per harmonic, fc1a–fc10d, s29–s68) were added to the data set.

Dissection procedures for siphonal structures: Five to eight randomly chosen segments per specimen were decalcified in a 20% HCl solution and rinsed in tap water. From the central-axial region of the segment, a long and relatively narrow piece, extending into the preceding segment over the node connecting both segments was excised (Fig. 2, c, 1). The cortex was scraped away from the excised fragment with a scalpel. The cortex piece was then placed on a microscope slide to yield a surface view. The medullar part that remained after removal of the cortex was prepared for examination as follows. For specimens belonging to section *Rhipsalis* (sensu Verbruggen and Kooistra 2004) the nodal region was sectioned longitudinally. Sections were placed on a microscope slide in clear Karo corn syrup diluted with water, and the siphons above and below the node were spread open using dissecting needles. For specimens belonging to the other sections, siphons were spread open so that nodal structure became clear. The cortex was examined in cavity slides using thick transverse cuts (Fig. 2, c, 2).

Medulla and node: From the medulla, seven types of measurements were taken (see Fig. 2d for a visualization and Table 4 for a list). Cell walls were included in the measurements. When connecting siphon segments were measured, the sequence in which they occurred was noted as well. The whole slide was screened for medullar ramifications; the fraction of dichotomous, trichotomous, and quadrichotomous ramifications was calculated from their counts.

Cortex: The surface diameter of peripheral utricles was measured from the scraped-off cortex part that was fixed in surface view. Another set of peripheral utricles was drawn in side view (camera lucida), and the utricles' length, width, and length-over-width ratio were computed from scanned images of these drawings (Fig. 2e). If peripheral utricles adhered to their neighbors, the height of the adhesion zone was recorded. For subperipheral utricles, we recorded length, diameter, the ratio between the former two, and the number of daughter utricles (Fig. 2e). Only the data for secondary and tertiary

TABLE 3. List of segment morphological variables.

	Variable	Description	Variable group
s1	dis_base	Location of the segment in the thallus: measured in no. of nodes from the basal segment	thallus structure variables
s2	thal_prt	Thallus part the segment is located in	
s3	apical	Is the segment apical? (binary variable)	
s4	calcif	Is the segment fully calcified? (binary variable)	
s5	no_sist	Number of sister segments	
s6	no_daugh	Number of daughter segments	
s7	form_seg	Categorical segment form: reniform, ovate, elliptical, obovate, cuneate, rectangular	categorical shape variables
s8	seg_widt	Categorical variable for relative segment width: narrow, medium, broad	
s9	stalk	Categorical variable describing the proximal stalk zone: absent, intermediate, present	
s10	form_bas	Categorical variable for the form of the segment base: auriculate to acute in five steps	
s11	lobedne	Categorical variable describing the segment's lobedness: absent, shallow, medium, deep	
s12	numlobes	Number of lobes:1 to 6 (six meaning many)	
s13	length	Segment length (mm); L_length is neperian logarithm hereof	conventional measurements
s14	width	Segment width (mm); L_width is neperian logarithm hereof	
s15	attach	Width of attachment zone (mm); L_attach is neperian logarithm hereof	
s16	homw	Height of maximal segment width (mm); L_homw is neperian logarithm hereof	
s17	thick	Segment thickness (mm); L_thick is neperian logarithm hereof	
s18	len_wd	Relative segment width: length-over-width ratio	ratio shape variables
s19	att_wd	Relative width of attachment zone: attach-over-width ratio	
s20	homw_len	Relative height of maximal width: homw-over-length ratio	
s21	thk_len	Relative segment thickness: thickness-over-length ratio	
s22	thk_att	Ratio of segment thickness over the width of the attachment zone	
s23	pw_uniX	Uniform shape change score X	partial warp scores
s24	pw_uniY	Uniform shape change score Y	
s25	pw_1X	Partial warp score 1X	
s26	pw_1Y	Partial warp score 1Y	
s27	pw_2X	Partial warp score 2X	
s28	pw_2Y	partial warp score 2Y	
s29-s68	fc1a-10d	Set of 40 Fourier coefficients (10 harmonics, 4 series)	Fourier

utricles was retained for analysis (variables a17–a23 for secondary utricles and a24–a30 for tertiary utricles). If measured utricles were connected to each other, their sequence in the series was noted.

Where possible, at least 10 replicate measurements (per segment) were made (e.g. measurements on 10 random peripheral utricles). These replicate measurements were averaged to yield a single value for each segment. All anatomical observations were made with a BX51 light microscope (Olympus Europe, Hamburg, Germany).

Statistical analyses. Taxonomic utility of the data: To test the taxonomic utility of the data set as a whole and its separate components, discriminant analyses (DAs) were performed using the GDA module of Statistica 6.0 (StatSoft Inc., Tulsa, OK, USA) with *a priori* groups corresponding to species clusters found in the molecular phylogeny. The percentage of correctly classified segments in DA was used as a measure of taxonomic power. Assumptions for DA were met except for some cases of heteroscedasticity. Because DA is fairly robust against violation of the homoscedasticity assumption (Lachenbruch 1975, Klecka 1980), in particular when violation is not due to outliers (which was not the case in our data), we further disregarded this assumption. Multicollinearity issues are touched on in Results. Segments from the basal thallus region and apical and noncalcified segments were excluded from all DAs (Verbruggen et al. 2005).

Segment morphology: Classification success of six DA models was compared. These models differed in the variable sets they included (conventional size, ratio shape sensu stricto + partial warp scores, Fourier coefficients, and combinations of these; see Fig. 4 for a complete list of combinations used). All effects were entered at once, prior probabilities were set to equal, and cross-validation was set so that 50% randomly chosen segments were used to build the model and the remaining segments were used to evaluate it. This procedure was repeated 20 times with different randomizations of segments used for model building and for testing. First, models were built to yield maximal separation of all nine species in the study (hereafter called nine-species models/analyses). Afterward, models were built for maximal separation of (closely related) taxa within individual sections (*H. macroloba* vs. *H. borneensis*, *H. tuna* vs. *H. taenicola* vs. *H. lacunalis*, and *H. opuntia* vs. *H. goreauii*; hereafter called within-section models/analyses). Because the data set of categorical shape variables was incomplete, we tested its taxonomic utility separately, on a subset of the data. Classification success of DA models based on categorical variables was compared with that of models based on ratio shape variables, partial warp scores, and Fourier coefficients. Additional models, embodying categorical variables and ratio shape variables or Fourier coefficients, were built and compared with models in which a single variable set was used.

Anatomy: Similarly for the anatomical data, a DA approach was used to determine the utility of the different variables. Anatomical structures not present in all nine species were omitted from nine-species analyses (basic models). For

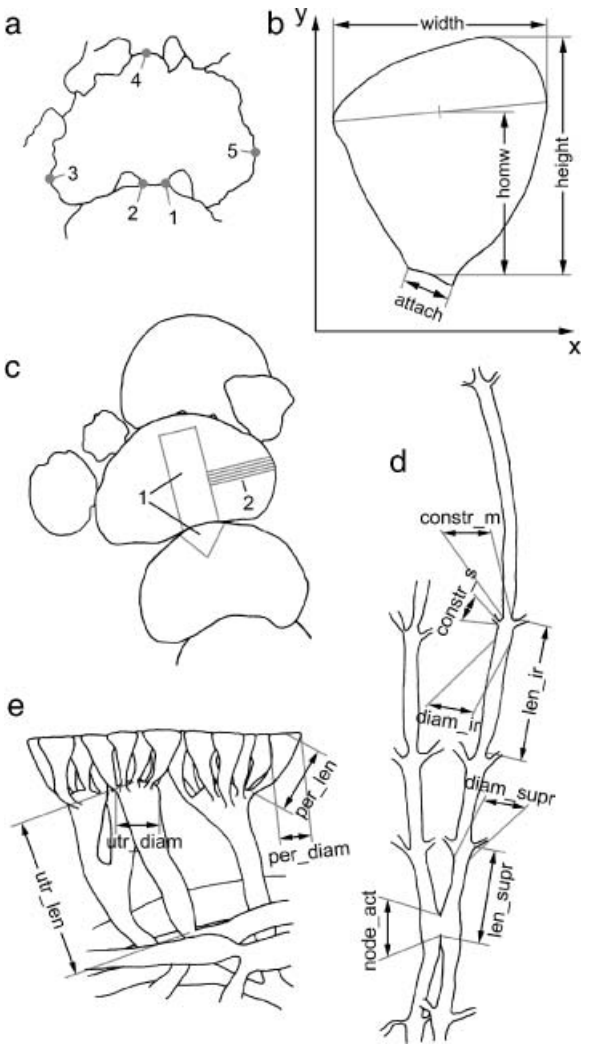

FIG. 2. Explanation of methods. (a) Digitized landmarks. (b) Size properties of segments as calculated from the landmark coordinates. The fifth segment size variable, thickness, is not shown. (c) Dissection of a segment. The gray lines illustrate the part cut out for node dissection (1) and the slices made for observations of the cortex (2). (d) Measurements made on medullar structures. (e) Measurements made on cortical structures. In the case shown here, utr_len and utr_diam (general notation used during data acquisition) correspond to sec_len and sec_diam, respectively (because it concerns a secondary utricle). The variable per_surf is not shown.

these analyses, we used four variable groups and different combinations of these groups: 1) the medullar, a1–a6; 2) the nodal zone, a9 and a10; 3) the peripheral utricles, a12–a15; and 4) the subperipheral utricles, a17-a20. Discriminant analyses were performed in a non–stepwise manner with equal prior probabilities and without cross-validation. For some within-section models, additional variables could be included (extended models). For DAs within sections *Rhipsalis* and *Opuntia*, actual node height (a11) was added to the models with nodal variables. Peripheral utricle models were expanded with the distance over which utricles adhere (a16). Finally, within-section models were expanded with the tertiary utricle variables a24–a27 for sections *Rhipsalis* and *Opuntia*.

Redundancy between anatomical variables within variable groups was traced using principal components analysis biplots and r^2 values of their linear regressions. One of both variables in the well-fitting linear regressions was subsequently left out of the discriminant models described above to evaluate its influence on classification success. Between-variable-group redundancy was examined by running canonical correlation analyses of all pairs of variables sets.

Sampling segments for anatomical investigation: Of all three representatives of *H. taenicola* in this study, five segments were dissected and 10 within-segment replicate measurements of each of the anatomical variables were taken. The data set comprising all 150 measurements per structure was considered to represent the statistical population. Four types of randomized subsets were created from the original data by retaining different numbers of specimens, numbers of segments per species, and/or numbers of replicate measurements per segment. The properties of the four subset types, together with their abbreviations, are listed in Table 5. Per subset type, 50 random subsets were created using self-written algorithms. In choosing which types of subsets to compare, we strived for equal total measuring effort (Table 5, fourth column). The anatomical variables examined were a1–a5, a9, and a12–a15.

After calculating the Euclidean distances between the means and SDs of the different subsets and those of the statistical population, patterns in these distances were visualized with the aid of mean and whisker plots. To test for differences between different segment sampling strategies, one-way analysis of variance tests and Tukey HSD post-hoc tests (Zar 1999) were carried out.

RESULTS

Molecular phylogeny, species identification, and the morphometric data set. Figure 3 presents 1 of 105 equally most parsimonious trees. Bootstrap values larger than 50 are indicated below branches. The phylogeny supports the five sections of the genus sensu Verbruggen and Kooistra (2004) and illustrates the representation of each of these five sections in our morphometric study (gray boxes). All specimens used in our morphometric analyses fell within existing species clades or were closely associated sisters to them. For all but two specimens, morphology- and sequence-based identifications corresponded. Only specimens HV183b and HV18-1 keyed out as *H. simulans* but clustered within the *H. borneensis* clade. We followed Kooistra et al. (2002) in their opinion that these look-alike species are geographically restricted and cling to the *H. borneensis* denomination for these Indo-Pacific specimens.

Of the 21 specimens listed in Table 1, 1346 segments were digitized. For each of these segments, values for 62 variables related to morphology and local thallus structure were generated (6 thallus structure variables, 5 size variables, 5 ratio variables, 6 partial warp scores, 40 Fourier coefficients). An additional six categorical variables were coded for a subset of 536 segments. In total, 104 segments were dissected. This resulted in measurements being taken of 2193 utricles (of which 1008 were peripheral), 982 medullar siphon branches, and 827 nodal structures.

Taxonomic utility: matrix ill-conditioning. Discriminant analysis reported matrix ill-conditioning (problematic levels of multicollinearity) when multiple variable

TABLE 4. List of anatomical variables.

	Variable	Description	Variable group
a1	len_ir	Distance between two subsequent ramifications (μm)	medullar properties
a2	diam_ir	Medullary siphon diameter (μm)	
a3	l_d_ir	Length-over-diameter ratio of the siphon segment: len_ir/dia_ir	
a4	constr_m	Constriction of main branch diameter (μm)	
a5	constr_s	Constriction of side branch diameter (μm)	
a6	frac_di	Fraction dichotomous ramifications	
a7	frac_tri	Fraction trichotomous ramifications	
a8	frac_qua	Fraction quadrichotomous ramifications	
a9	len_supr	Distance from below node to supranodal ramification (μm)	nodal properties
a10	diam_supr	Thickness of the supranodal interramification (μm)	
a11	node_act	Actual pore size or node height (μm)	
a12	per_surf	Surface diameter peripheral utricle (μm)	peripheral utricles
a13	per_len	Length (height) of peripheral utricle (μm)	
a14	per_diam	Diameter of peripheral utricle (μm)	
a15	per_l_d	Relative length of the peripheral utricle: per_len over per_diam ratio	
a16	per_adh	Distance over which peripheral utricles adhere (μm)	
a17	sec_len	Length (μm) of the secondary utricle	secondary utricles
a18	sec_diam	Maximal diameter (μm) of the secondary utricle	
a19	sec_l_d	Relative length of secondary utricle: sec_len over sec_diam ratio	
a20	sec_2_succ	Fraction of measured secondary utricles carrying two peripheral utricles	
a21	sec_3_succ	Fraction of measured secondary utricles carrying three peripheral utricles	
a22	sec_4_succ	Fraction of measured secondary utricles carrying four peripheral utricles	
a23	sec_5p_succ	Fraction of measured secondary utricles carrying five or more peripheral utricles	
a24	ter_len	Length (μm) of the tertiary utricle	tertiary utricles
a25	ter_diam	Maximal diameter (μm) of the tertiary utricle	
a26	ter_l_d	Relative length of tertiary utricle: ter_len over ter_diam ratio	
a27	ter_2_succ	Fraction of measured tertiary utricles carrying two secondary utricles	
a28	ter_3_succ	Fraction of measured tertiary utricles carrying three secondary utricles	
a29	ter_4_succ	Fraction of measured tertiary utricles carrying four secondary utricles	
a30	ter_5p_succ	Fraction of measured tertiary utricles carrying five or more secondary utricles	

groups were combined in one predictive model. Initial analyses pointed out that a number of variables could be discarded without loss of discriminative power. Segment size variability was efficiently captured by two variables, the log-transforms of segment length and thickness. Furthermore, partial warp scores proved to be closely related to ratio variables; many of them showed nearly perfect correlations (Verbruggen et al. 2005; Fig. 1). Therefore, these two variable sets were merged and a number of ratios (s18–s20) were excluded from all further analyses. Their notation in Figures 4 and 5 is "ratio s.s. + landmark." For DAs based on anatomical data, multicollinearity was not an issue of importance.

TABLE 5. Summary of the different subset types created to assess how their means and SDs approximate that of the statistical population.

Specimens	Segments	Replicates	Total replicates	Abbreviation
2	1	10	20	2-1-10
1	2	10	20	1-2-10
2	2	5	20	2-2-5
3	1	7	21	3-1-7

The first column lists the number of (randomly chosen) specimens retained in the subset. The second column specifies how many segments were randomly chosen from each of the specimens. The third column lists the number of replicate measurements taken from each of the segments. The fourth and fifth columns list the total sample size (total number of replicates) and the abbreviation of the subset type used throughout the text. This abbreviation consists of a series of three numbers representing (in this order) the content of column 1, 2, and 3.

Segment morphology. Classification success in DA varied strongly between species and methods. The models' performance was poor for species of section one (*H. macroloba* and *H. borneensis*). Rather than being misclassified within the lineage, their segments were most often mistaken for segments of section *Halimeda* species. For the other species, classification success was considerably higher. The upper graph of Figure 4 shows the overall classification success for the six combinations of morphometric variables used. The percentage correctly classified segments varied between 50% and 70%. Of the individual variable sets, Fourier coefficients performed best. The combination of ratio shape variables and partial warp scores had the poorest differentiating power. All models with more than one variable group showed significantly more correct allocations. Nevertheless, results were far from additive, indicating considerable redundancy between variable sets. Including Fourier coefficients in any of these nine-species models significantly increased its taxonomic power.

When the success of classification into species groups was examined within each of the sections separately, patterns somewhat different from those observed previously were obtained. These within-section

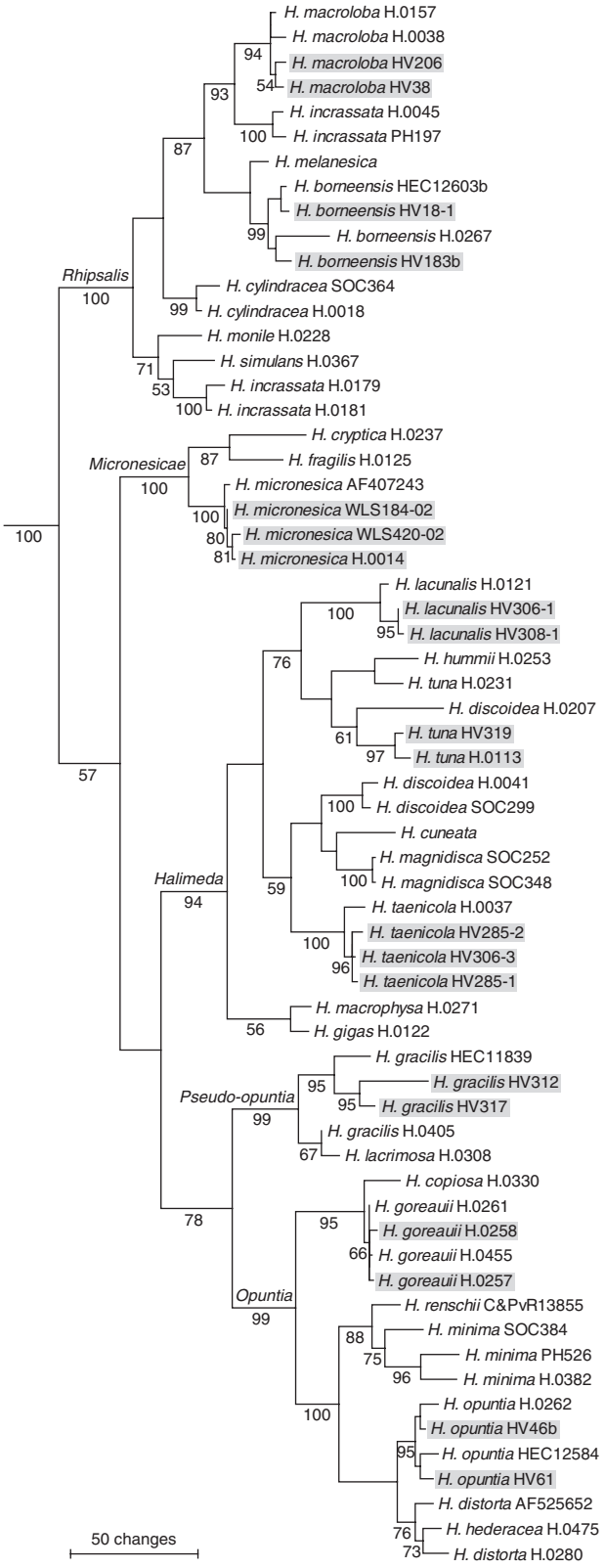

FIG. 3. Phylogeny of *Halimeda* taxa used in this study. One of 105 most parsimonious trees (1506 steps). Maximum parsimony bootstrap values >50 are indicated below and section names above internodes. The outgroup taxa were removed from the tree. Taxa used in the morphometric study are in gray boxes.

patterns were highly uniform for the three sections examined. The lower graph of Figure 4 shows the taxonomic power of the different models for section *Halimeda* (*H. lacunalis*, *H. taenicola*, and *H. tuna*). Compared with nine-species models, overall classification success was higher, and the contribution of the different variable sets to the taxonomic power of the model differed. The most remarkable difference is that adding Fourier coefficients to a model now decreased its taxonomic power, whereas in nine-species models this always led to an increase in classification success.

We also assessed the taxonomic utility of the categorical shape variables, using the subset of data for which these variables were available (Fig. 5). On average, categorical variables scored 47.5% correct classifications, significantly less than any other model tested. The combination of ratio variables (sensu stricto) and partial warps scored somewhat higher, but it was Fourier coefficients and models incorporating several variable sets that performed best. When categorical shape predictors were combined with ratio shape variables and partial warps or with Fourier coefficients

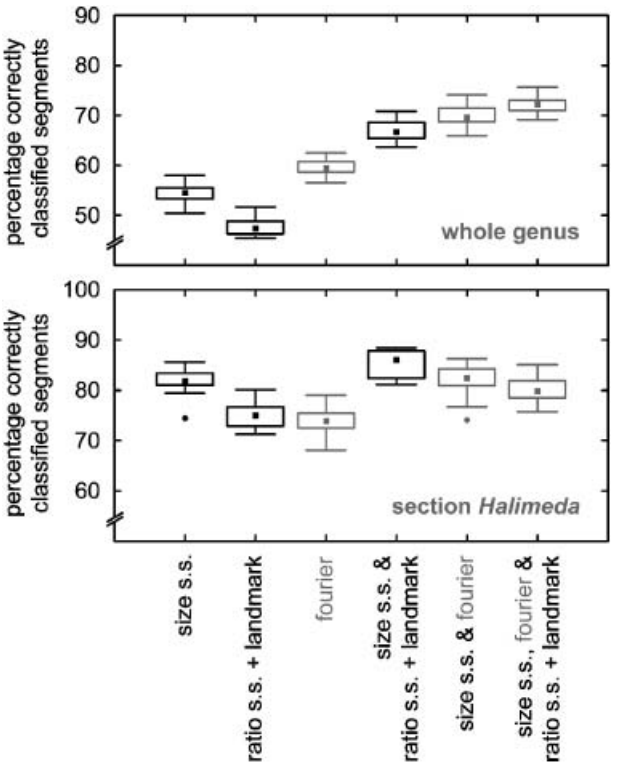

FIG. 4. Classification success of DA models constructed using different combinations of segment morphological variables (abscissa). The graphs depict the percentage of segments that were assigned to the species to which they belong. In the upper graph, the DA models were built for maximal discrimination between species within the whole genus; in the lower graph, only species belonging to section *Halimeda* were retained for DA. Models containing Fourier coefficients are in gray. The central squares indicate median values, the boxes are the 25 percentiles, the whiskers refer to nonoutlier range, and the outer dots represent outliers.

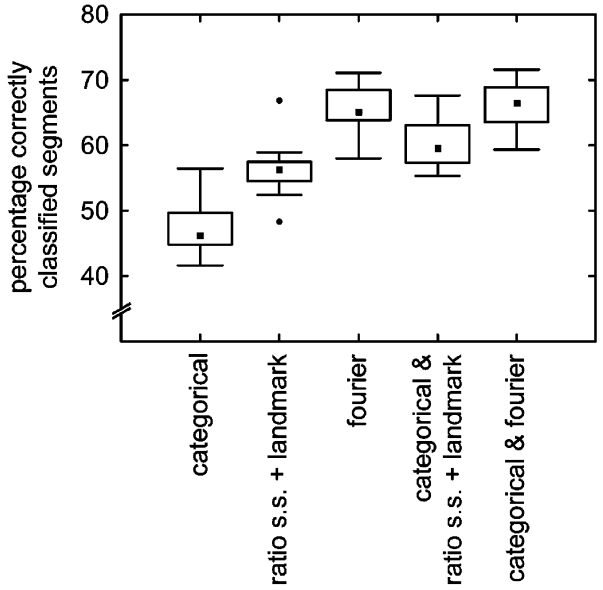

FIG. 5. DA with categorical segment shape descriptors. The different combinations of segment morphological variables used in the DA models are indicated along the abscissa. The graphs depict the percentage of segments that were assigned to the species group to which they belong. The central dots indicate median values, the boxes are the 25 percentiles, the whiskers refer to nonoutlier range, and the outer dots represent outliers.

(last two cases in Fig. 5), it became clear that categorical variables added power to the DA model based on ratio shape variables but not to that based on Fourier coefficients. The significance levels of the differences between simple models and models enriched with categorical shape predictors were <0.001 and 0.999 for the ratio and landmark model and the Fourier model, respectively (Tukey HSD test).

Anatomy. Table 6 summarizes the results of the anatomy-based predictive discriminant models. Overall classification success was high: Models based on more than one variable group always yielded more than 90% correct classifications. In nine-species models, segments were most often misclassified as a species belonging to another section rather than to the same section. An examination of the factor structures of the models indicated that the different diameter measures of medullar and cortical siphons had a high differentiating power. The anatomy model (7) had primary and secondary roots with high loadings of the cortical variables, indicating their relative importance for discriminating between species at this taxonomic level. Within-section predictive DA always exceeded 90% classification success; models with more than one variable group even resulted in 100% correct allocations (except for one model in section *Halimeda*).

The results of the reruns of DAs without some of the strongly correlated variables were not uniform throughout the genus but generally resulted in a decrease of discriminatory power. As an example we

TABLE 6. Classification success of the DA models based on anatomical data, given as the percentage of segments assigned to the species group they actually belong to.

	Nine species	Section *Rhipsalis*	Section *Halimeda*	Section *Opuntia*
1, medullar structures	87.3	100	87.0	100
2, nodal structures	58.7	b:91.7 e:100	82.6	b:90.9 e:100
3, peripheral utricles	84.1	b:100 e:100	b:91.3 e:91.3	b:100 e:100
4, subperipheral utricles	69.8	b:91.7 e:91.7	87.0	b:90.9 e:100
5, medulla s.l. (1–2)	90.5	b:100 e:100	100	b:100 e:100
6, cortex (3–4)	93.7	b:100 e:100	95.6	b:100 e:100
7, anatomy (1–4)	100	b:100 e:100	100	b:100 e:100

For certain individual sections, different b and e scores are given. These letters stand for basic models (including only variables measurable throughout the whole genus) and extended models (including variables measurable in this section but not throughout the genus), respectively.

elaborate the results for the set of medullar variables. Internal redundancy in this variable set was high. The first two principal components represented 80% of the total variability in the data. Variables a4, a5, and a6 clustered close together in the biplot. For nine-species analyses, the DA model with all medullar (s.s.) variables included yielded a classification success of 87.3%. Leaving out variable a5 reduced this value to 84.1%, whereas omitting variables a4 or a6 had stronger effects (reduction to 76.2% and 79.4%, respectively). With both variables a5 and a6 left out, classification success was 79.4%. For analyses within sections *Opuntia* or *Rhipsalis*, there were no observable effects of leaving out any of the variables a4, a5, and a6 or any of their combinations. In section *Halimeda*, however, classification success was left unaffected when omitting variables a4 or a6, whereas leaving out a5 resulted in a slight increase from 87.0% to 91.3%. Removal of variable a3, which had low loadings on the roots of the different models, reduced classification success from 87.3% to 81.0% for nine-species models and did not alter the performance of within-section models.

Redundancy between variable groups was evident as well. Canonical analyses run between each two sets of anatomical variables revealed that between 28% and 70% of the variability within one variable set was accounted for by the other variable set. Mutual redundancy of variable groups based on similar structures and on locally adjacent structures was higher.

Sampling segments for anatomical investigation. The upper graph of Figure 6 depicts the distances between the mean values of the different subsets and the statistical population. The lower graph of Figure 6 shows the distances for the SDs. The patterns shown in these graphs were representative of those found for most variables studied. Both for means (upper graph) and SDs (lower graph), the *y* values of

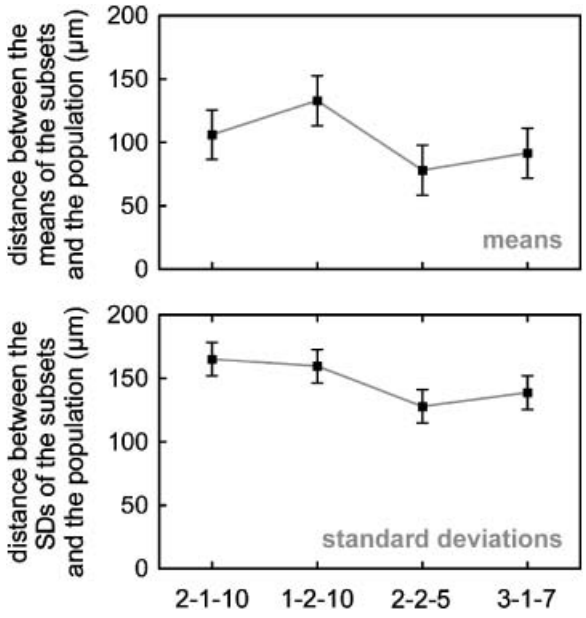

FIG. 6. The upper graph shows the Euclidean distances between the mean values of the variable diam_ir for the different types of subsets described in Table 5 and the mean of the statistical population. The lower graph depicts the Euclidean distances between the SDs of the variable diam_ir for the different types of subsets and the SD of the statistical population. The filled square and whiskers represent the mean distance±1 SD for the population of 50 random subsets of each given type.

the 2-1-10 and 1-2-10 sampling strategies were higher than those of the 2-2-5 and 3-1-7 sampling methods. These differences were, however, generally nonsignificant (Tukey HSD tests). For the most part, the distances from the population score were significantly different (higher) only for the second sampling method (1-2-10).

DISCUSSION

The days that *Halimeda* species were described solely on the basis of what their segments looked like lie far behind us. Soon after taxonomists started examining the anatomy of the thalli (Askenasy 1888), they realized that this was the key to a firm taxonomy, and the first measurements of anatomical structures appeared in literature (Barton 1901, Howe 1907). With both revisions of Hillis (1959, Hillis-Colinvaux 1980), even more emphasis was placed on anatomical characters. Molecular studies have now unveiled that these anatomical characters have not engendered an evolutionary correct classification (Kooistra et al. 2002, Verbruggen and Kooistra 2004). For example, the species *H. incrassata*, *H. copiosa*, and *H. discoidea* each consist of two unrelated species (Kooistra et al. 2002). Furthermore, within the species *H. minima*, *H. tuna*, and the *H. distorta* complex, significant phylogenetic structure indicates cryptic species diversity (Kooistra et al. 2002, Verbruggen and Kooistra 2004, Kooistra and Verbruggen 2005). Verbruggen and Kooistra (2004) advocated the use of quantitative morphological characters in taxonomical analyses. The method presented in the present study, which unites molecular information and morphometric data of segments and anatomy, permits distinction of the different species with high accuracy.

Segment morphology was regarded by Hillis-Colinvaux (1980) as an "exceedingly variable character" of limited utility in *Halimeda* systematics. Where used in taxonomy, segments are typified only by simple linear measurements and a descriptive expression of shape. Our results show that linear measurements are good predictors of species membership (Fig. 4). Shape descriptors, whether based on ratios of linear measurements or on geometric morphometric analyses, are in themselves of slightly lower taxonomic utility. When shape and size information are combined, DA models can pinpoint optimally to which species a specimen belongs.

Categorical shape variables, coding characters used in traditional taxonomy, are no match for morphometric variable sets. But here again, models incorporating both types of data performed best. An interesting result in this context was that adding categorical variables to different discriminant models had discrepant outcomes. For the ratio- and landmark-based discriminant model, higher classification success was achieved, whereas no effect was observed for the DA model based on Fourier coefficients. This is not surprising: the five landmarks on which ratio shape variables are based (Fig. 2a) were unable to capture certain segment properties that are embodied by the categorical shape variables (e.g. auriculate base, presence of a stalk). Conversely, Fourier coefficients are based on complete outlines of segments and are able to capture all properties coded in the categorical shape variables.

Comparing nine-species and within-section analyses yields information on the contrasts in performance of discriminant models in broad- versus narrow-scale taxonomy. The most important result in this context was that nine-species models reacted positively to the addition of Fourier coefficients, whereas within-section designs reacted negatively. Yet it is obvious that models solely based on Fourier coefficients achieved higher levels of classification success than those based solely on ratio shape variables and partial warps on both taxonomic scales. The latter finding implies that Fourier coefficients hold taxonomically useful information that is not present in the ratio shape variables or partial warps. But then why do within-section models enriched with Fourier coefficients perform worse than their more basic counterparts? In part, this is because those shape attributes coded in Fourier coefficients and not in the other shape data sets are largely uninformative at this taxonomic level. Furthermore, variables inherently incorporate a certain amount of noise and, in our case, lead to enhanced levels of multicollinearity. Therefore, adding a substantial amount of variables to discriminant models can lead to a reduction of their performance by lowering the accuracy

and/or precision of regression coefficient estimation (Grapentine 1997).

In the progression of *Halimeda* studies, it was soon conceived that ecological factors can have a strong influence on segment morphology and that, for solving taxonomic issues, emphasis could better be placed on anatomical characters. At first, attention was paid to nodal fusion patterns (Barton 1901). Cortex structure and utricle dimensions soon followed as prime characters for species delineation (Barton 1901, Howe 1907). We did not include structural patterns in our analyses; instead, we concentrated on the dimensions of the different anatomical structures. Our results support the notion that anatomical information is a valuable species delineator. Classification success increased with expansion of the predictor variable content of the models, often reaching 100% in within-section analyses. The achievements and the buildup of the models show that cortical variables (particularly utricle length and diameter) have a high discriminative potential. This result justifies the importance traditional taxonomists attached to these measurements.

Optimization of the procedures. One of the missions of this study was to attain a time-efficient protocol for future case studies by reducing the number of methods applied and measurements taken while maintaining the achievement of predictive DAs. Our results provide clear information on which methods and measurements to abandon for narrow-scale investigations. The reduction of within-section classification success after addition of Fourier coefficients suggests that outline analysis can be dropped without devaluating the taxonomy-beneficial information content of the data. In addition to this, EFA is labor intensive because segment outlines have to be traced manually. Automatic detection is virtually impossible because segments are often superimposed and cannot be distinguished by a brightness threshold. Furthermore, the attachment zone between mother and daughter segments is hard to detect automatically. Isolating segments would solve these problems but is, because of its destructive nature, unjustifiable when using historic or rare herbarium materials.

The process of excluding variables from the anatomical data was not as straightforward as it was for the morphological data. In spite of the fact that redundancy levels were high and that discarding certain variables did not substantially alter the classification success, results were not homogenous throughout the phylogenetic spectrum of the genus. Only the width of medullar side branches at their constriction appears superfluous throughout all lineages within the genus and is thus eligible for exclusion from future studies.

Despite not being able to eliminate a subset of anatomical measurements, time-efficiency of anatomical data gathering can be substantially improved. Our analysis of the behavior of central and deviance measures of a number of representative anatomical variables as a function of specimen and segment sampling approaches, although possibly impeded by small sampling size, indicates that dissecting fewer segments per specimen and more specimens per population better approximates the variability found within that population than dissecting more segments per specimen from a small number of specimens. Because dissecting and preparing a segment is approximately equally time consuming as measuring 10 replicates of all anatomical structures in the slide, reducing the number of segments per specimen is a time saver. Of course, when picking out a limited amount of segments per specimen, this should be done minimizing the risk of those segments being deviant. Consequently, apical segments, noncalcified segments, and segments from the basal thallus region should be precluded (Verbruggen et al. 2005).

Perspectives. The molecular phylogenetic studies of Kooistra point out several groups of species that require additional taxonomic attention (Kooistra et al. 1999, 2002). It mostly concerns phylogenetically distant look-alikes with fuzzy species delineations (e.g. *H. borneensis–simulans*, *H. copiosa–hederacea*) and morphospecies that are nonmonophyletic (e.g. *H. incrassata*, *H. discoidea*, *H. tuna*, *H. gracilis*) or embody cryptic diversity (e.g. *H. minima*, *H. hederacea–distorta* complex). Traditional taxonomic practices have provided insufficient arguments to lead to an evolutionary correct classification of the phyletic entities within each of these species groups. It is self-evident that this does not imply the absence of morphological differences between the phyletic entities. On the contrary, subtle anatomical differences between genetically distinct entities of *H. tuna* and *H. discoidea* were observed (Hillis 1959, Hillis-Colinvaux 1980). These findings strengthen our belief that a morphometric approach embodying precise measurements and thorough statistical analyses can aid the taxonomy of each of the problematic morphocomplexes.

In this context, the application of DAs on morphometric data, with *a priori* groups defined on the basis of molecular data, opens a variety of perspectives. First, it permits evaluating whether species differences actually exist. This can be evaluated by means of multivariate analysis of variance (or nonparametric alternatives) or by checking whether the number of accurate designations in DA exceeds that expected by chance alone. Second, it allows pinpointing morphometric variables that provide strong differentiating power. These variables can then be translated into diagnostic characters by which specimens can be identified. Alternatively, a computer-assisted identification system could be established. This system could be trained (calibrated) using the existing database of segment pictures. Via automated contour extraction of digitized isolated segments, new specimens could then be identified using an automated classification procedure (e.g. neural networks). Our results indicate that for such an approach to yield high levels of correct classification, several segments per specimen must be included.

The present study used within-section DAs to estimate the feasibility of morphometric taxonomy of closely related species. The high levels of adequate group membership prediction are promising for actual case studies. Nonetheless, two things must be stressed here. First, the sample size of this study was far too small to draw firm taxonomic conclusions. Adding specimens will undoubtedly increase the ranges of most variables and consequently alter the DA models. Second, species sampling in this study did not include actual problem clades. To some extent this limits the value of the predictive extrapolation toward puzzling morphocomplexes, but, on the other hand, the broad-scale sampling presented here is essential for the development of a sound morphometric modus operandi.

Not only does the finding that morphometrics allows species identification in our data set appear to be promising for future taxonomic case studies in extant representatives, it also pleads for a more standardized approach of the *Halimeda* fossil record. Of particular interest are the ambiguous species ages. Kooistra et al. (2002) estimated these to be less than 3 million years, whereas several paleontological studies report extant species from Miocene (Dragastan et al. 2002), Eocene (Dragastan and Soliman 2002), and Cretaceous (Dragastan et al. 2002, and references therein) deposits. Meticulous morphometric comparisons of extant and fossil *Halimeda* specimens could be used as additional information in this matter.

Finally, we wish to broaden the discussion toward Bryopsidalean algae. Within individual genera of this group, basic anatomical architecture is fairly homogeneous, whereas finer structural elements exhibit variation that is considered to be taxonomically useful (Silva 1959a,b, Ducker 1967, Farghaly and Denizot 1979, Olsen-Stojkovich 1985, Kraft 1986, Littler and Littler 1990, 1992, Krellwitz et al. 2001, de Senerpont Domis et al. 2003). On the other hand, traditional morphotaxonomic insights have been refuted by phylogenetic studies (Kooistra 2002, Kooistra et al. 2002). Recent morphometric studies on Bryopsidalean algae (Krellwitz et al. 2001, Hubbard and Garbary 2002, de Senerpont Domis et al. 2003, this study, unpublished data) prove that the combination of architectural constancy and fine-structural variability within genera permits establishing a morphometric method that is applicable to a variety of species yet provides accurate taxonomic resolution. In conclusion, most current evidence agrees that the shaky species-level taxonomy of Bryopsidalean algae benefits from studies founded on a combination of molecular phylogenetics and statistically founded morphometrics.

H. V. is indebted to the Bijzonder Onderzoeksfonds (Ghent University, grant 011D9101) and O. D. C to the Fund for Scientific Research Flanders (grant 3G002496 and postdoctoral research grant). P. Colinvaux, L. Hillis, A. N'Yeurt, and G. Procaccini are acknowledged for specimen collection. H. V. thanks C. Payri, P. Vanai, and the Environmental Service of Wallis and Futuna for facilitating fieldwork on Uvea Island. The comments from the associate editor M. Kamiya and two anonymous referees are greatly appreciated.

Askenasy, E. 1888. Algen. *In Die Forschungsreise S. M. S*. Gazelle Th. 4, Bot., Berlin.

Ballantine, D. L. 1982. *Halimeda hummii* sp. nov., *Halimeda cryptica* v. *acerifolia* var. nov. (Caulerpales, Chlorophyta), and additional records of *Halimeda* species from Puerto Rico. *J. Phycol.* 18:86–91.

Barton, E. S. 1901. *The Genus Halimeda. Monographs of the Siboga Expedition* 60. Brill Leiden, The Netherlands, 32 pp.

Bookstein, F. L. 1989. Principal warps: thin-plate splines and the decomposition of deformations. *IEEE T. Pattern Anal.* 11:567–85.

Bookstein, F. L. 1991. *Morphometric Tools for Landmark Data*. Cambridge University Press, Cambridge, UK, 435 pp.

Bookstein, F. L. 1996. Standard formula for the uniform shape component in landmark data. *Adv. Morphometr.* 284:153–68.

Borowitzka, M. A. & Larkum, A. D. W. 1977. Calcification in the green alga *Halimeda*. V. An ultrastructure study of the thallus development. *J. Phycol.* 13:6–16.

Collado-Vides, L. 2002. Morphological plasticity of *Caulerpa prolifera* (Caulerpales, Chlorophyta) in relation to growth form in a coral reef lagoon. *Bot. Mar.* 45:123–9.

Dargent, O. 1997. *Etude systématique du genre Halimeda (Caulerpales, Bryopsidophycées), dans la zone de contact entre l'Océan Indien et l'Océan Pacifique*. M.Sc. thesis, Université Pierre et Marie Curie (Paris VI), Paris, France, 30 pp.

de Senerpont Domis, L. N., Famà, P., Bartlett, A. J., Prud'homme van Reine, W. F., Armenta-Espinosa, C. & Trono, G. C. Jr 2003. Defining taxon boundaries in members of the morphologically and genetically plastic genus *Caulerpa* (Caulerpales, Chlorophyta). *J. Phycol.* 39:1019–37.

Dong, M. & Tseng, C. K. 1980. Studies on some marine green algae from the Xisha Islands, Guandong Province, China. II. *Stud. Mar. Sin.* 17:1–10.

Dragastan, O. N., Littler, D. S. & Littler, M. M. 2002. Recent vs. fossil *Halimeda* species of Angaur Island, Palau and adjacent western Pacific areas. Acta Palaeontologica romaniae, Special publication no.1, Cartea Universitara, University of Bucharest, Bucharest, Romania, 20 pp.

Dragastan, O. N. & Soliman, H. A. 2002. Paleogene calcareous algae from Egypt. *Micropaleontology* 48:1–30.

Ducker, S. C. 1967. The genus *Chlorodesmis* (Chlorophyta) in the Indo-Pacific region. *Nova Hedw.* 13:145–82.

Farghaly, M. S. & Denizot, M. 1979. Le genre *Rhipiliopsis*. Définition et place dans les Caulerpales (Chlorophycées). *Rev. Algol.* 14:169–84.

Grapentine, T. 1997. Managing multicollinearity: real-world survey data can create surrealistic analytic models. Grapentine Company On-line Publications. http://www.grapentine.com/articles/multicol.pdf

Hall, T. A. 1999. BioEdit: a user-friendly biological sequence alignment editor and analysis program for Windows 95/98/NT. Version 5.0.9. *Nucleic Acids. Symp. Ser.* 41:95–8.

Haywood, A. J., Steidinger, K. A., Truby, E. W., Bergquist, P. R., Bergquist, P. L., Adamson, J. & MacKenzie, L. 2004. Comparative morphology and molecular phylogenetic analysis of three new species of the genus *Karenia* (Dinophyceae) from New Zealand. *J. Phycol.* 40:165–79.

Hillis, L. W. 1959. A revision of the genus *Halimeda* (order Siphonales). *Publ. Inst. Mar. Sci.* 6:321–403.

Hillis-Colinvaux, L. 1980. Ecology and taxonomy of *Halimeda*: primary producer of coral reefs. *Adv. Mar. Biol.* 17:1–327.

Howe, M. A. 1907. Phycological studies. III. Further notes on *Halimeda* and *Avrainvillea* (pro parte: Halimeda). *Bull. Torrey Bot. Club* 34:491–516.

Hubbard, C. B. & Garbary, D. J. 2002. Morphological variation of *Codium fragile* (Chlorophyta) in Eastern Canada. *Bot. Mar.* 45:476–85.

Isaev, M. 1995. *EFAWin. Windows Shell for EFA*. Free for download from http://life.bio.sunysb.edu/morph/

Kamiya, M., Zuccarello, G. C. & West, J. A. 2003. Evolutionary relationships of the genus *Caloglossa* (Delesseriaceae, Rhodophyta)

inferred from large-subunit ribosomal RNA gene sequences, morphological evidence and reproductive compatibility, with description of a new species from Guatemala. *Phycologia* 42: 478–97.

Klecka, W. R. 1980. *Discriminant Analysis*. Sage, Beverly Hills, CA, 71 pp.

Kooistra, W. H. C. F. 2002. Molecular phylogenies of Udoteaceae (Bryopsidales, Chlorophyta) reveal nonmonophyly for *Udotea*, *Penicillus* and *Chlorodesmis*. *Phycologia* 41:453–62.

Kooistra, W. H. C. F., Caldéron, M. & Hillis, L. W. 1999. Development of the extant diversity in *Halimeda* is linked to vicariant events. *Hydrobiologia* 398:39–45.

Kooistra, W. H. C. F., Coppejans, E. G. G. & Payri, C. 2002. Molecular systematics, historical ecology and phylogeography of *Halimeda* (Bryopsidales). *Mol. Phylogenet. Evol.* 24:121–38.

Kooistra, W. H. C. F. & Verbruggen, H. 2005. Genetic patterns in the calcified tropical seaweeds *Halimeda opuntia*, *H. distorta*, *H. hederacea*, and *H. minima* (Bryopsidales, Chlorophyta) provide insights in species boundaries and interoceanic dispersal. *J. Phycol.* 41:177–87.

Kraan, S., Rueness, J. & Guiry, M. D. 2001. Are North Atlantic *Alaria esculenta* and *A. grandifolia* (Alariaceae, Phaeophyceae) conspecific? *Eur. J. Phycol.* 36:35–42.

Kraft, G. T. 1986. The green algal genera *Rhipiliopsis* A. & E. S. Gepp and *Rhipiliella* gen. Nov. (Udoteaceae, Bryopsidales) in Australia and the Philippines. *Phycologia* 25:47–72.

Kraft, G. T. 2000. Marine and estuarine benthic algae (Chlorophyta) of Lord Howe Island, South-western Pacific. *Austral. Syst. Bot.* 13:509–648.

Krellwitz, E. C., Kowallik, K. V. & Manos, P. S. 2001. Molecular and morphological analyses of *Bryopsis* (Bryopsidales, Chlorophyta) from the western North Atlantic and Caribbean. *Phycologia* 40:330–9.

Kuhl, F. P. & Giardina, C. R. 1982. Elliptic Fourier features of a closed contour. *Comput. Graph. Image Process.* 18:236–58.

Lachenbruch, P. A. 1975. *Discriminant Analysis*. Hafner Press, New York, 128 pp.

Littler, D. S. & Littler, M. M. 1990. Systematics of *Udotea* species (Bryopsidales, Chlorophyta) in the tropical western Atlantic. *Phycologia* 29:206–52.

Littler, D. S. & Littler, M. M. 1992. Systematics of *Avrainvillea* (Bryopsidales, Chlorophyta) in the tropical western Atlantic. *Phycologia* 31:375–418.

Murray, S., Jorgensen, M. F., Daugbjerg, N. & Rhodes, L. 2004. *Amphidinium* revisited. II. Resolving species boundaries in the *Amphidinium operculatum* species complex (Dinophyceae), including the descriptions of *Amphidinium trulla* sp nov and *Amphidinium gibbosum* comb. nov. *J. Phycol.* 40:366–82.

Noble, J. M. 1986. *Halimeda magnidisca* (Caulerpales, Chlorophyta), a new species from the Great Barrier Reef, Australia. *Phycologia* 25:331–9.

Noble, J. M. 1987. *A Taxonomic Study of the Genus Halimeda Lamouroux (Chlorophyta, Caulerpales) From the Heron Island Region of the Southern Great Barrier Reef, Australia*. Masters degree thesis, University of Melbourne, Melbourne, Australia, 200 pp.

Olsen-Stojkovich, J. 1985. A systematic study of the genus *Avrainvillea* Decaisne (Chlorophyta, Udoteaceae). *Nova Hedw.* 41:1–68.

Rohlf, F. J. 1993. Relative warp analysis and an example of its application to mosquito wings. *In* Marcus, L. F., Bello, E. & Garcia-Valdecasas, A. [Eds.] *Contributions to Morphometrics*. Vol. 8. Museo Nacional de Ciencias Naturales (CSIC), Madrid, Spain, pp. 131–59.

Rohlf, F. J. 1998. *tpsSMALL*. Version 1.19. State University of New York at Stony Brook, Stony Brook, NY. Downloadable from http://life.bio.sunysb.edu/morph/

Rohlf, F. J. 2001a. *tpsDIG*. Version 1.31. State University of New York at Stony Brook, Stony Brook, NY. Free for download from http://life.bio.sunysb.edu/morph/

Rohlf, F. J. 2001b. *tpsRELW*. Version 1.31. State University of New York at Stony Brook, Stony Brook, NY. Free for download from http://life.bio.sunysb.edu/morph/

Rohlf, F. J., Loy, A. & Corti, M. 1996. Morphometric analysis of old world Talpidae (Mammalia, Insectivora) using partial-warp scores. *Syst. Biol.* 45:344–62.

Rohlf, F. J. & Marcus, L. M. 1993. A revolution in morphometrics. *Trends Ecol. Evol.* 8:129–32.

Rohlf, F. J. & Slice, D. E. 1990. Extensions of the Procrustes method for the optimal superimposition of landmarks. *Syst. Zool.* 39:40–59.

Sherwood, A. R. & Sheath, R. G. 1999. Biogeography and systematics of *Hildenbrandia* (Rhodophyta, Hildenbrandiales) in North America: inferences from morphometrics and *rbc*L and 18S rRNA gene sequence analyses. *Eur. J. Phycol.* 34:523–32.

Slice, D. E. 2000. *Morpheus et al. Software for Morphometric Research*. Beta version of 01/31/2000. Free for download from http://life.bio.sunysb.edu/morph/morpheus/

Silva, P. C. 1959a. The genus *Codium* (Chlorophyta) in South Africa. *J. S. Afr. Bot.* 15:103–65.

Silva, P. C. 1959b. *Codium* (Chlorophyta) in the tropical Western Atlantic. *Nova Hedw.* 1:497–536.

Swofford, D. L. 2001. *PAUP* Phylogenetic Analysis Using Parsimony (*and Other Methods)*. Version 4.0.b10. Sinauer Associates Inc., Sunderland, MA.

Verbruggen, H., De Clerck, O. & Coppejans, E. 2005. Deviant segments hamper a morphometric approach towards *Halimeda* taxonomy. *Cryptog. Algol.* Volume 26 (in press).

Verbruggen, H. & Kooistra, W. H. C. F. 2004. Morphological characterization of lineages within the calcified tropical seaweed genus *Halimeda* (Bryopsidales, Chlorophyta). *Eur. J. Phycol.* 39: 213–28.

Vieira, J. & Necchi, O. 2002. Microhabitat and plant structure of Characeae (Chlorophyta) populations in streams from Sao Paulo State, southeastern Brazil. *Cryptog. Algol.* 23:51–63.

Vroom, P. S. & Smith, C. M. 2003. Reproductive features of Hawaiian *Halimeda velasquezii* (Bryopsidales, Chlorophyta), and an evolutionary assessment of reproductive characters in *Halimeda*. *Cryptog. Algol.* 24:355–70.

Vroom, P. S., Smith, C. M., Coyer, J. A., Walters, L. J., Hunter, C. L., Beach, K. S. & Smith, J. E. 2003. Field biology of *Halimeda tuna* (Bryopsidales, Chlorophyta) across a depth gradient: comparative growth, survivorship, recruitment, and reproduction. *Hydrobiologia* 501:149–66.

Zar, J. H. 1999. *Biostatistical Analysis*. 4th ed. Prentice-Hall, Upper Saddle River, NJ, 663 pp.